

This is the peer reviewed version of the following article:

Qualitative graphical representation of Nyquist plots / Zanasi, Roberto; Grossi, Federica; Biagiotti, Luigi. - In: SYSTEMS & CONTROL LETTERS. - ISSN 0167-6911. - STAMPA. - 83:(2015), pp. 53-60. [10.1016/j.sysconle.2015.06.005]

Terms of use:

The terms and conditions for the reuse of this version of the manuscript are specified in the publishing policy. For all terms of use and more information see the publisher's website.

24/04/2026 22:14

(Article begins on next page)

Qualitative Graphical Representation of Nyquist Plots

R. Zanasi^a, F. Grossi^{a,*}, L. Biagiotti^a

^a*Department of Engineering “Enzo Ferrari”,
University of Modena and Reggio Emilia, via Pietro Vivarelli 10, 41125 Modena, Italy*

Abstract

In this paper, the procedure for manually drawing the Nyquist plot of a generic transfer function is revised and, in particular, two novel parameters (Δ_τ , Δ_p), which allow to simplify this process, are presented. Thanks to these parameters, the analysis of the frequency response at low and high frequencies is considerably enhanced, with a very little effort. These parameters allow to predict initial and final directions of the polar curve in the vicinity of initial and final points and consequently the sectors of the complex plane where the plot starts/ends. In many cases it is possible to obtain a qualitative Nyquist plot, able to correctly predict the stability properties of the closed-loop system, by simply joining the initial and final tracts found with the proposed procedure. Moreover, the analysis based on these parameters can aid to correctly interpret the plots obtained with computer programs which often, in particular when poles at the origin are present, hide the behavior of the frequency response in the area close to the origin of the complex plane.

Keywords: Nyquist plot, Frequency response, Stability analysis.

1. Introduction

In classical control theory, Nyquist stability criterion plays a central role for discussing the stability of closed-loop systems. Its effectiveness is strictly related

*Corresponding author

Email addresses: roberto.zanasi@unimore.it (R. Zanasi),
federica.grossi@unimore.it (F. Grossi), luigi.biagiotti@unimore.it (L. Biagiotti)

to the correct drawing of the polar plots of the loop transfer function $G(j\omega)$. However, in many applications the exact plot is not essential and a rough sketch reproducing the shape of the polar plot of $G(j\omega)$ may be sufficient, provided that this plot correctly reproduces the encirclements of the loop transfer function about the critical point $-1+j0$ and the intersections with the real axis. The rules for drawing Nyquist plots seem well settled and are illustrated in all controls textbooks with no substantial differences, see e.g. [1, 2, 3] among many others. They are based on the analytical computation of the frequency response $G(j\omega)$ for $\omega = 0$, $\omega = \infty$ and for those frequencies where the diagram intersects the real and imaginary axes. In more complex cases, i.e. high-order systems, polar plots are obtained indirectly, by means of a sort of “translation” of Bode diagrams in the polar plane. Unfortunately, standard approaches are characterized by some drawbacks. They may require complex calculations. Moreover, an analysis based on Bode diagrams (with the phase starting/ending at an integer multiple of $\pi/2$) may lead to the wrong conclusion that the polar plots always start from or end to a point located in the real or imaginary axis (see for instance the figures reported in textbook [2], and in particular Fig. 8-33). Indeed, as highlighted by [4], when the polar plots start at infinity the locus generally does not approach a coordinate axis but tends to get further and further away from these axes.

The use of CACSD (Computer Aided Control System Design) programs is the option that provides the best results in terms of accuracy. But, also in these cases some problems may arise. In fact, often the obtained polar plots may result unreadable because of the large span in the magnitude over the entire frequency range, that hides the local behavior of the curve, in particular in the region enclosed by the unit circle. This situation is quite common when systems owning poles on the imaginary axis are considered. In order to cope with this problem in [5, 6] a logarithmic scaling of the magnitude of the frequency response is proposed, that allows to magnify the parts of the polar plot close to the origin without losing the diagram overview. This approach gives good results in particular with respect to the problem of detecting the intersection with

the (negative) real axis, but it is characterized by two important drawbacks: the proposed plotting technique needs a numerical analysis software (Matlab functions have been developed by the authors) and it requires to arbitrarily set the minimum value of the magnitude that can be represented in the diagram.

In this paper, the method for manually drawing polar plots is revised. The proposed approach has a great value from an educational point of view for a twofold reason. On the one hand, the definition of two novel parameters (Δ_τ , Δ_p) contributes to greatly simplify the drawing procedure and to improve the correctness of the Nyquist plot, in particular in the regions “far from” and “close to” the origin. On the other hand, these two parameters and the related considerations can also be the key to correctly interpret many polar plots obtained with CACSD programs. This allows to correctly analyze the stability of the system in a feedback configuration on the basis of the Nyquist criterion. Moreover, the use of parameters Δ_τ and Δ_p can be useful to study the dynamic behavior of a linear system in feedback configuration with a nonlinear static element. In this case, these parameters used together with well-known methods such as circle criterion [7], Popov criterion [7] or describing function method [8], may be conclusive to assess the stability of the nonlinear feedback system.

The paper is organized as follows. In Sec. 2 the proposed parameters for a qualitative evaluation of Nyquist plots are defined and their meaning explained. In Sec. 3 the method for drawing Nyquist plots by exploiting the proposed parameters is illustrated step by step, and some numerical examples are provided in Sec. 4. Concluding remarks are given in the last section.

2. Qualitative graphical analysis of the frequency response in the complex plane

Consider a transfer function $G(s)$, without time-delays, expressed as follows

$$G(s) = \frac{\mathcal{K}}{s^h} \frac{\prod_{i=1}^p (\beta_{i,m_i} s^{m_i} + \beta_{i,m_i-1} s^{m_i-1} + \dots + \beta_{i,1} s + \beta_{i,0})}{\prod_{i=1}^q (\alpha_{i,n_i} s^{n_i} + \alpha_{i,n_i-1} s^{n_i-1} + \dots + \alpha_{i,1} s + \alpha_{i,0})}, \quad (1)$$

where $\alpha_{i,0} \neq 0$, $\beta_{i,0} \neq 0$, $\sum_{i=1}^p m_i = m$ and $\sum_{i=1}^q n_i = n$. Note that from (1) it is possible to obtain all the standard expressions of rational polynomial transfer functions, i.e.

- Polynomial form $G(s) = \frac{b_m s^m + b_{m-1} s^{m-1} + \dots + b_1 s + b_0}{s^h (a_n s^n + a_{n-1} s^{n-1} + \dots + a_1 s + a_0)}$
- Zero-pole-gain form $G(s) = \rho \frac{(s - z_1)(s - z_2) \cdots (s - z_m)}{s^h (s - p_1)(s - p_2) \cdots (s - p_n)}$
- Time-constant form $G(s) = \mu \frac{(1 + \tau'_1 s)(1 + \tau'_2 s) \cdots (1 + \tau'_m s)}{s^h (1 + \tau_1 s)(1 + \tau_2 s) \cdots (1 + \tau_n s)}$

2.1. Approximating functions

The initial and final points of the polar plot can be obtained by considering the functions $G_0(s)$ and $G_\infty(s)$ that approximate $G(s)$ for $|s| \simeq 0^+$ and $|s| \simeq \infty$, respectively. The approximating function $G_0(s)$ is obtained from $G(s)$ in (1) by neglecting all the s terms except for zeros and poles at the origin:

$$G_0(s) = \lim_{|s| \simeq 0^+} G(s) = \frac{\mu}{s^h} \quad \text{where} \quad \mu = \mathcal{K} \frac{\prod_{i=1}^p \beta_{i,0}}{\prod_{i=1}^q \alpha_{i,0}}. \quad (2)$$

The function $G_\infty(s)$ is deduced from $G(s)$ in (1) by considering in the numerator and denominator polynomials only the polynomials of s of higher degree, i.e.

$$G_\infty(s) = \lim_{|s| \simeq \infty} G(s) = \frac{\rho}{s^r} \quad \text{where} \quad \rho = \mathcal{K} \frac{\prod_{i=1}^p \beta_{i,m_i}}{\prod_{i=1}^q \alpha_{i,n_i}} \quad (3)$$

where $r = h + n - m$ is the relative degree of function $G(s)$. The start-point and the end-point of the polar plot, denoted respectively with $q_0 = M_0 e^{j\varphi_0}$ and $q_\infty = M_\infty e^{j\varphi_\infty}$, can be computed by considering the magnitude and the phase of the frequency responses $G_0(j\omega)$ and $G_\infty(j\omega)$ for $\omega \rightarrow 0^+$ and $\omega \rightarrow \infty$:

$$M_0 = \lim_{\omega \rightarrow 0^+} \frac{|\mu|}{\omega^h} = \begin{cases} \infty & \text{if } h > 0 \\ |\mu| & \text{if } h = 0 \\ 0 & \text{if } h < 0 \end{cases}, \quad \varphi_0 = \arg(\mu) - h \frac{\pi}{2}$$

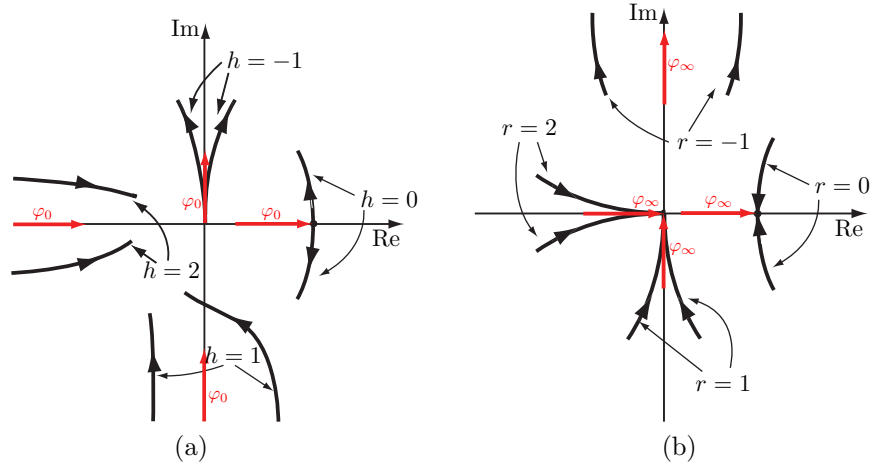


Figure 1: Polar plots in the low frequency range when $\rho > 0$ for different values of h (a) and plots in the high frequency range when $\mu > 0$ for different values of the relative degree r (b).

$$M_\infty = \lim_{\omega \rightarrow \infty} \frac{|\rho|}{\omega^r} = \begin{cases} 0 & \text{if } r > 0 \\ |\rho| & \text{if } r = 0 \\ \infty & \text{if } r < 0 \end{cases}, \quad \varphi_\infty = \arg(\rho) - r \frac{\pi}{2}$$

where $\arg(\mu)$ and $\arg(\rho)$ are 0 or $-\pi$ according to the sign, positive or negative, of the constants μ and ρ . Therefore, as well-known, for $\omega \rightarrow 0^+$ polar plots start from the origin if $h < 0$, from a point of the real axis if $h = 0$, or from infinity if $h > 0$, see Fig. 1(a). Dually, for $\omega \rightarrow \infty$ Nyquist plots end to infinity if $r < 0$, in a point of the real axis if $r = 0$ or into the origin if $r > 0$, see Fig. 1(b). The initial and final directions of the polar plot are determined by parameters φ_0 and φ_∞ . However, as shown in Fig. 1 for both $\omega \simeq 0^+$ and $\omega \simeq \infty$, the graphical behavior of the polar plot is not univocal because system $G(s)$ may exhibit a phase lead or a phase lag with respect to φ_0 and φ_∞ .

2.2. Low frequency behavior

In order to evaluate the initial phase shift of $G(s)$, it is necessary to take into account the contribution of all the poles and zeros of the system. From the

generic transfer function $G(s)$ given in (1), rewritten as follows

$$\begin{aligned} G(s) &= \frac{\mu}{s^h} \frac{\prod_{i=1}^p \left(\frac{\beta_{i,m_i}}{\beta_{i,0}} s^{m_i} + \frac{\beta_{i,m_i-1}}{\beta_{i,0}} s^{m_i-1} + \dots + \frac{\beta_{i,1}}{\beta_{i,0}} s + 1 \right)}{\prod_{i=1}^q \left(\frac{\alpha_{i,n_i}}{\alpha_{i,0}} s^{n_i} + \frac{\alpha_{i,n_i-1}}{\alpha_{i,0}} s^{n_i-1} + \dots + \frac{\alpha_{i,1}}{\alpha_{i,0}} s + 1 \right)} \\ &= \frac{\mu}{s^h} \tilde{G}_0(s) = G_0(s) \tilde{G}_0(s) \end{aligned}$$

it is possible to derive a first order approximation of $G(s)$ for low frequencies by expanding function $\tilde{G}_0(s)$ in Taylor series at $s = 0$, i.e.

$$G(s) = \frac{\mu}{s^h} \left(\tilde{G}_0(s) \Big|_{s=0} + \frac{d\tilde{G}_0(s)}{ds} \Big|_{s=0} s + o(s^2) \right) \simeq \frac{\mu}{s^h} \left(1 + \frac{d\tilde{G}_0(s)}{ds} \Big|_{s=0} s \right) = G'_0(s)$$

Since the derivative of function $\tilde{G}_0(s)$ can be expressed as

$$\begin{aligned} \frac{d\tilde{G}_0(s)}{ds} &= \tilde{G}_0(s) \left(\sum_{i=1}^p \frac{m_i \frac{\beta_{i,m_i}}{\beta_{i,0}} s^{m_i-1} + (m_i-1) \frac{\beta_{i,m_i-1}}{\beta_{i,0}} s^{m_i-2} + \dots + \frac{\beta_{i,1}}{\beta_{i,0}}}{\frac{\beta_{i,m_i}}{\beta_{i,0}} s^{m_i} + \frac{\beta_{i,m_i-1}}{\beta_{i,0}} s^{m_i-1} + \dots + \frac{\beta_{i,1}}{\beta_{i,0}} s + 1} \right. \\ &\quad \left. - \sum_{i=1}^q \frac{n_i \frac{\alpha_{i,n_i}}{\alpha_{i,0}} s^{n_i-1} + (n_i-1) \frac{\alpha_{i,n_i-1}}{\alpha_{i,0}} s^{n_i-2} + \dots + \frac{\alpha_{i,1}}{\alpha_{i,0}}}{\frac{\alpha_{i,n_i}}{\alpha_{i,0}} s^{n_i} + \frac{\alpha_{i,n_i-1}}{\beta_{i,0}} s^{n_i-1} + \dots + \frac{\alpha_{i,1}}{\alpha_{i,0}} s + 1} \right) \end{aligned}$$

it follows that the approximation of $G(s)$ for low frequencies is

$$G(s)|_{s \simeq 0} \simeq G'_0(s) = \frac{\mu}{s^h} (1 + \Delta_\tau s) \quad (4)$$

where

$$\Delta_\tau = \frac{d\tilde{G}_0(s)}{ds} \Big|_{s=0} = \sum_{i=1}^p \frac{\beta_{i,1}}{\beta_{i,0}} - \sum_{i=1}^q \frac{\alpha_{i,1}}{\alpha_{i,0}}. \quad (5)$$

When $G(s)$ is expressed in one of the standard forms reported at the beginning of the section, the parameter Δ_τ can be easily computed as follows

$$\begin{aligned} \Delta_\tau &= \frac{b_1}{b_0} - \frac{a_1}{a_0}, & \text{for polynomial form} \\ \Delta_\tau &= -\sum_{i=1}^m \frac{1}{z_i} + \sum_{i=1}^n \frac{1}{p_i}, & \text{for zero-pole-gain form} \\ \Delta_\tau &= \sum_{i=1}^m \tau'_i - \sum_{i=1}^n \tau_i, & \text{for time-constant form.} \end{aligned}$$

Note that symbol Δ_τ comes from the last relation: when $G(s)$ is in time-constant form the parameter Δ_τ is the difference between the time constants τ_i of the

zeros and τ'_i of the poles of the transfer function $G(s)$. However, it is also worth noticing that when the values of the zeros/poles or the equivalent time constants are not available the computation of Δ_τ can be performed by directly using the coefficients of the polynomial form, see (5).

Remark 1. Consider the transfer function

$$G_T(s) = G(s)T(s) \quad (6)$$

where $G(s)$ is a rational function, as given in (1), and $T(s)$ is a non-rational function, e.g. a time-delay or more generally a transfer function describing an infinite dimensional system in the Laplace domain. The parameter Δ_τ for system $G_T(s)$ can be computed as follows

$$\Delta_\tau = \sum_{i=1}^p \frac{\beta_{i,1}}{\beta_{i,0}} - \sum_{i=1}^q \frac{\alpha_{i,1}}{\alpha_{i,0}} + \delta_\tau \quad (7)$$

where

$$\delta_\tau = \lim_{\omega \rightarrow 0} \frac{1}{T(s)} \Big|_{s=j\omega} \frac{dT(s)}{ds} \Big|_{s=j\omega}.$$

Relation (7) can be used only if parameter δ_τ is finite. In the case of a time-delay system it is $T(s) = e^{-t_0 s}$ and $\delta_\tau = -t_0$.

Theorem 1. For $\omega \simeq 0^+$, the phase shift of $G(j\omega)$ with respect to φ_0 is given by $\Delta\varphi_0 = \Delta_\tau \omega$. Therefore $\Delta_\tau > 0$ implies an initial phase lead $\Delta\varphi_0 > 0$ and $\Delta_\tau < 0$ implies an initial phase lag $\Delta\varphi_0 < 0$.

PROOF. The frequency response of the approximating function $G'_0(s)$ in (4) is

$$G(j\omega)|_{\omega \simeq 0^+} \simeq G'_0(j\omega) = \frac{\mu}{(j\omega)^h} [1 + j\omega\Delta_\tau] \quad (8)$$

and the argument of $G(j\omega)$ for $\omega \simeq 0^+$ is

$$\begin{aligned} \arg G(j\omega)|_{\omega \simeq 0^+} &\simeq \arg(\mu) - h\frac{\pi}{2} + \arctan(\Delta_\tau\omega) \\ &\simeq \varphi_0 + \Delta_\tau\omega \end{aligned} \quad (9)$$

where the approximation $\arctan(x) \simeq x$ for $x \simeq 0$ has been considered. \square

If $\Delta_\tau = 0$ the Nyquist plot starts tangentially to the coordinate axis defined by φ_0 . In this case, the initial phase shift $\Delta\varphi_0$ can be estimated by expanding the function $\tilde{G}_0(s)$ in a third-order Taylor series at $s = 0$, but, because of the complexity of the involved computations, this result has no practical interest.

Theorem 2. *For system with $h > 0$, the Nyquist plot starts from infinity. When $h = 1$, the plot is tangent to a vertical asymptote whose abscissa is $\sigma_0 = \mu \Delta_\tau$, while when $h > 1$ no asymptotes exist.*

PROOF. From (8) it is possible to conclude that

- if $h = 0$, $\lim_{\omega \rightarrow 0^+} G(j\omega) = \mu$;
- if $h = 1$, $\lim_{\omega \rightarrow 0^+} \operatorname{Re}\{G(j\omega)\} = \mu \Delta_\tau$ and $\lim_{\omega \rightarrow 0^+} \operatorname{Im}\{G(j\omega)\} = \infty$;
- if $h > 1$, $\lim_{\omega \rightarrow 0^+} \operatorname{Re}\{G(j\omega)\} = \infty$ and $\lim_{\omega \rightarrow 0^+} \operatorname{Im}\{G(j\omega)\} = \infty$ but no linear asymptotes exist¹. □

2.3. High frequency behavior

To predict the behavior of $G(s)$ for high frequencies, it is useful to rewrite the transfer function $G(s)$ as follows

$$\begin{aligned} G(s) &= \frac{\rho}{s^r} \frac{\prod_{i=1}^p \left(\frac{\beta_{i,0}}{\beta_{i,m_i}} \frac{1}{s^{m_i}} + \frac{\beta_{i,1}}{\beta_{i,m_i}} \frac{1}{s^{m_i-1}} + \dots + \frac{\beta_{i,m_i-1}}{\beta_{i,m_i}} \frac{1}{s} + 1 \right)}{\prod_{i=1}^q \left(\frac{\alpha_{i,0}}{\alpha_{i,n_i}} \frac{1}{s^{n_i}} + \frac{\alpha_{i,1}}{\alpha_{i,n_i}} \frac{1}{s^{n_i-1}} + \dots + \frac{\alpha_{i,n_i-1}}{\alpha_{i,n_i}} \frac{1}{s} + 1 \right)} \\ &= \frac{\rho}{s^r} \tilde{G}_\infty(s) = G_\infty(s) \tilde{G}_\infty(s). \end{aligned}$$

Let $\tilde{G}_\infty(p) = \tilde{G}_\infty(s)|_{s=\frac{1}{p}}$ denote the following function

$$\tilde{G}_\infty(p) = \frac{\prod_{i=1}^p \left(\frac{\beta_{i,0}}{\beta_{i,m_i}} p^{m_i} + \frac{\beta_{i,1}}{\beta_{i,m_i}} p^{m_i-1} + \dots + \frac{\beta_{i,m_i-1}}{\beta_{i,m_i}} p + 1 \right)}{\prod_{i=1}^q \left(\frac{\alpha_{i,0}}{\alpha_{i,n_i}} p^{n_i} + \frac{\alpha_{i,1}}{\alpha_{i,n_i}} p^{n_i-1} + \dots + \frac{\alpha_{i,n_i-1}}{\alpha_{i,n_i}} p + 1 \right)}.$$

¹When $h > 1$, from (8) it follows that the cartesian expression of the polynomial curve in the complex plane that approximates $G(j\omega)$ for $\omega \simeq 0^+$ is $\operatorname{Re}\{G(j\omega)\}^h = \operatorname{Const} \cdot \operatorname{Im}\{G(j\omega)\}^{h-1}$ if h is odd or $\operatorname{Im}\{G(j\omega)\}^h = \operatorname{Const} \cdot \operatorname{Re}\{G(j\omega)\}^{h-1}$ if h is even, see [4].

Since the Taylor series expansion of function $\tilde{G}_\infty(s)$ at $s = \infty$ is equal to the series expansion of function $\tilde{G}_\infty(p)$ at $p = 0$, the first order approximation of function $G(s)$ at $s = \infty$ can be written as follows

$$G(s)|_{s \simeq \infty} \simeq \frac{\rho}{s^r} \left(\tilde{G}_\infty(p)|_{p=0} + \left. \frac{d\tilde{G}_\infty(p)}{dp} \right|_{p=0} p \right) = \frac{\rho}{s^r} \left(1 - \frac{\Delta_p}{s} \right) = G'_\infty(s) \quad (10)$$

where

$$\Delta_p = \left. \frac{d\tilde{G}_\infty(p)}{dp} \right|_{p=0} = \sum_{i=1}^q \frac{\alpha_{i,n_i-1}}{\alpha_{i,n_i}} - \sum_{i=1}^p \frac{\beta_{i,m_i-1}}{\beta_{i,m_i}}. \quad (11)$$

Expression (11) is obtained directly from (5) noting that function $\tilde{G}_\infty(p)$ shares the same structure of function $\tilde{G}_0(s)$ with inverted coefficients: $j \rightarrow (m_i - j)$ at numerator and $j \rightarrow (n_i - j)$ at denominator. When $G(s)$ is expressed in one of the standard forms, the parameter Δ_p can be computed as follows:

$$\begin{aligned} \Delta_p &= \frac{a_{n-1}}{a_n} - \frac{b_{m-1}}{b_m}, & \text{for polynomial form} \\ \Delta_p &= \sum_{i=1}^n z_i - \sum_{i=1}^m p_i, & \text{for zero-pole-gain form} \\ \Delta_p &= \sum_{i=1}^n \frac{1}{\tau_i} - \sum_{i=1}^m \frac{1}{\tau_i}, & \text{for time-constant form.} \end{aligned}$$

In this case the symbol Δ_p is due to the fact that Δ_p is the difference between zeros and poles of the transfer function $G(s)$.

Remark 2. Consider the transfer function $G_T(s)$ given in (6) and let $T(p) = T(s)|_{s=\frac{1}{p}}$. In this case the parameter Δ_p in (11) must be modified as follows

$$\Delta_p = \left. \frac{d\tilde{G}_\infty(p)}{dp} \right|_{p=0} = \sum_{i=1}^q \frac{\alpha_{i,n_i-1}}{\alpha_{i,n_i}} - \sum_{i=1}^p \frac{\beta_{i,m_i-1}}{\beta_{i,m_i}} + \delta_p \quad (12)$$

where

$$\delta_p = \lim_{\omega \rightarrow 0} \frac{1}{T(p)} \bigg|_{p=j\omega} \frac{dT(p)}{dp} \bigg|_{p=j\omega}. \quad (13)$$

Relation (12) can be used only if parameter δ_p is finite. For time-delay systems $T(s) = e^{-t_0 s}$ the parameter δ_p cannot be used because in (13), where $T(p) = e^{-\frac{t_0}{p}}$ and $\frac{dT(p)}{dp} = \frac{t_0}{p^2} e^{-\frac{t_0}{p}}$, the limit for $\omega \rightarrow 0$ does not exist.

Theorem 3. For $\omega \simeq \infty$ the phase shift of $G(j\omega)$ with respect to φ_∞ is given by $\Delta\varphi_\infty = \Delta_p \frac{1}{\omega}$. Therefore $\Delta_p > 0$ implies a final phase lead $\Delta\varphi_\infty > 0$ and $\Delta_p < 0$ implies a final phase lag $\Delta\varphi_\infty < 0$.

PROOF. The frequency response of the approximating function $G'_\infty(s)$ in (10) is

$$G(j\omega)|_{\omega \simeq \infty} \simeq G'_\infty(j\omega) = \frac{\rho}{(j\omega)^r} \left(1 + j\frac{1}{\omega}\Delta_p \right) \quad (14)$$

and the argument of $G(j\omega)$ in the high frequency range can be expressed as

$$\begin{aligned} \arg G(j\omega)|_{\omega \simeq \infty} &\simeq \arg(\rho) - r\frac{\pi}{2} + \arctan\left(\Delta_p \frac{1}{\omega}\right) \\ &\simeq \varphi_\infty + \Delta_p \frac{1}{\omega}. \quad \square \end{aligned} \quad (15)$$

Similarly to Δ_τ , if $\Delta_p = 0$ it is not possible to determine the final phase shift of $G(j\omega)$ on the basis of a first-order Taylor series but it is necessary to consider a third-order approximation. In this case, the polar plot ends tangentially to the coordinate axis defined by φ_∞ .

Theorem 4. For system with $r < 0$, the Nyquist plot ends to infinity. When $r = -1$, the plot is tangent to a vertical asymptote with abscissa $\sigma_\infty = -\rho \Delta_p$, while when $r < -1$ no asymptotes exist.

PROOF. From (14) it is straightforward to conclude that

- if $r = 0$, $\lim_{\omega \rightarrow \infty} G(j\omega) = \rho$;
- if $r = -1$, $\lim_{\omega \rightarrow \infty} \operatorname{Re}\{G(j\omega)\} = -\rho \Delta_p$ and $\lim_{\omega \rightarrow \infty} \operatorname{Im}\{G(j\omega)\} = \infty$;
- if $r < -1$, $\lim_{\omega \rightarrow \infty} \operatorname{Re}\{G(j\omega)\} = \infty$ and $\lim_{\omega \rightarrow \infty} \operatorname{Im}\{G(j\omega)\} = \infty$ but no linear asymptotes exist². □

3. Qualitative drawing of the Nyquist plot

The qualitative drawing of the Nyquist plot of a generic transfer function $G(s)$ having the structure given in (1) can be done using the following procedure.

²When $r < -1$, from (14) it follows that the cartesian expression of the polynomial curve in the complex plane that approximates $G(j\omega)$ for $\omega \simeq \infty$ is $\operatorname{Re}\{G(j\omega)\}^r = \operatorname{Const} \cdot \operatorname{Im}\{G(j\omega)\}^{r+1}$ or $\operatorname{Im}\{G(j\omega)\}^r = \operatorname{Const} \cdot \operatorname{Re}\{G(j\omega)\}^{r+1}$ according to the value of r .

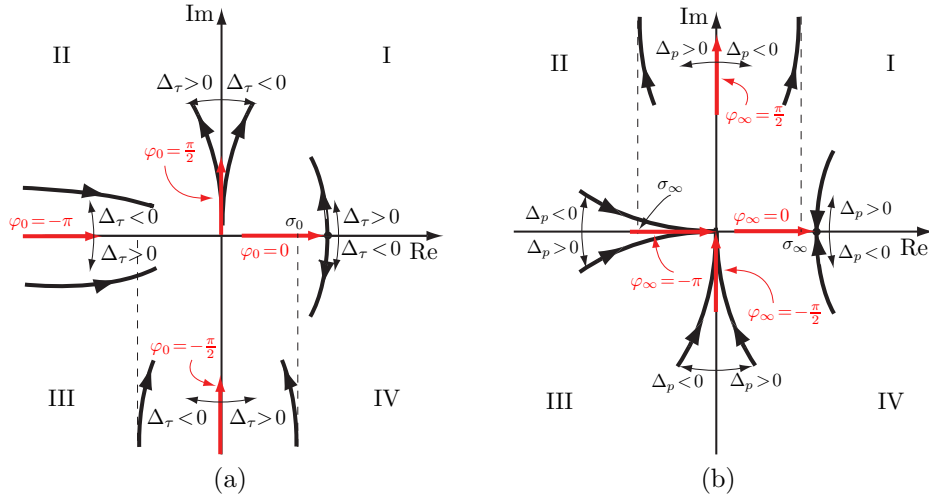


Figure 2: Low frequency (a) and high frequency (b) behaviors of the systems shown in Fig. 1 for positive and negative values of parameters Δ_τ and Δ_p , respectively.

1. Initial point. The initial point of the diagram can be determined by computing magnitude $M_0 = |G_0(j\omega)|$ and phase $\varphi_0 = \arg\{G_0(j\omega)\}$ of the approximating function $G_0(j\omega)$ for $\omega \rightarrow 0^+$.
2. Phase shift (lead or lag) for $\omega \simeq 0^+$. For $\omega \simeq 0^+$ the Nyquist plot starts with a phase shift $\Delta\varphi_0$ which is concordant with the sign of parameter Δ_τ defined in (5). Therefore, by using parameter Δ_τ it is possible to deduce in which quadrant the polar plot starts, see Fig. 2(a).
3. Final point. The final point of the diagram can be determined by computing magnitude $M_\infty = |G_\infty(j\omega)|$ and phase $\varphi_\infty = \arg\{G_\infty(j\omega)\}$ of the approximating function $G_\infty(j\omega)$ for $\omega \rightarrow \infty$.
4. Phase shift (lead or lag) for $\omega \simeq \infty$. For $\omega \simeq \infty$ the Nyquist plot ends with a phase shift $\Delta\varphi_\infty$ which is concordant with the sign of parameter Δ_p defined in (11). As shown in Fig. 2(b), by calculating Δ_p it is possible to find in which quadrant of the complex plane the ending segment of the polar plot is contained.
5. Presence of asymptotes. For systems with $h = 1$ the polar plot exhibits a vertical asymptote, for $\omega \rightarrow 0^+$, whose abscissa is $\sigma_0 = \mu\Delta_\tau$ as stated in Theorem 2. Dually, for systems with $r = -1$, the abscissa of the vertical asymptote for $\omega \rightarrow \infty$ is $\sigma_\infty = -\rho\Delta_p$, see Theorem 4. In all the other cases, no

asymptotes exist.

6. Total phase variation. When ω varies from 0^+ to ∞ , the rotation angle of $G(j\omega)$ about the origin can be calculated as

$$\Delta\varphi = -\frac{\pi}{2}(n_{p,s} - n_{p,u} - n_{z,s} + n_{z,u}) \quad (16)$$

where $n_{p,s}$, $n_{z,s}$, $n_{p,u}$ and $n_{z,u}$ denote the number of “stable” and “unstable” poles and zeros of function $G(s)$, respectively. Note that the computation of $\Delta\varphi$ only requires the knowledge of the amount of stable and unstable poles and zeros but not necessarily their numerical value. As a consequence, if poles and zeros are not explicitly given, e.g. when $G(s)$ is given in polynomial form, it is sufficient to apply the Routh-Hurwitz criterion to both numerator and denominator of the transfer function $G(s)$ to find $n_{p,s}$, $n_{z,s}$, $n_{p,u}$ and $n_{z,u}$.

7. Analytical computation of $G(j\omega)$ for some frequency values. A precise drawing of the Nyquist plot needs the exact computation of some peculiar points that belong to the curve. In particular, the intersections with the real axis are of great importance for many aims, including stability analysis of linear systems, stability margins evaluation, stability analysis of systems with static nonlinearities, etc. While a direct computation³ of such intersections may lead to complex calculations, the application of the Routh-Hurwitz stability criterion to the characteristic equation $1 + kG(s) = 0$ of the feedback system as a function of k provides a simple method for obtaining such intersections. As a matter of fact, if k^* denotes a value of the gain k which makes the system marginally stable, i.e. it nullifies an element of the first column of the Routh table, an intersection of the Nyquist plot with the real axis occurs in $G(j\omega) = -\frac{1}{k^*}$.

8. Nyquist plot drawing for ω from 0^+ to ∞ . Once that initial and final segments of the polar curve are known, the Nyquist plot can be obtained by connecting them with a continuous curve which performs a rotation of an angle $\Delta\varphi$ about the origin and crosses the real axis in correspondence of the points

³Usually the intersection with the real axis are deduced by computing $G(j\omega^*)$ for those angular frequencies ω^* which guarantee $\text{Im}\{G(j\omega^*)\} = 0$.

computed in the previous step. Obviously, the exact computation of some points contributes to improve the precision of the polar plot, but a qualitative sketch/analysis only based on initial and final directions and on the phase shift $\Delta\varphi$ may be sufficient for many goals including stability analysis, see Sec. 4.

9. Complete Nyquist plot. The frequency response for negative values of ω is the complex-conjugate of function $G(j|\omega|)$. Therefore, the Nyquist plot for ω ranging from $-\infty$ to 0^- can be deduced from that of $G(j\omega)$ obtained for positive values of ω by reflecting this plot with respect to the real axis. Finally, if the curve starts from infinity for $\omega \simeq 0$, i.e. $h > 0$, the complete Nyquist plot is obtained by connecting point $G(j0^-)$ with point $G(j0^+)$ with h clockwise semicircles of infinite radius. Dually, if the curve goes to infinity for $\omega \simeq \infty$, i.e. $r < 0$, the complete Nyquist plot is obtained by connecting point $G(+j\infty)$ with point $G(-j\infty)$ with r clockwise semicircles of infinite radius.

4. Numerical examples

In order to highlight the significance of the two parameters Δ_τ and Δ_p , a few examples, that appear in the literature⁴, have been taken into account. For the sake of simplicity, the considered transfer functions are supposed to be characterized by positive static gain μ and positive time constants τ'_i, τ_i , but it is worth noticing that the correctness of the proposed procedure does not depend on these conditions.

1. Consider the transfer function $G_1(s) = \mu \frac{(1 + \tau'_1 s)}{s^2 (1 + \tau_1 s) (1 + \tau_2 s)}$.

The initial and final points are characterized by

$$G_{1,0}(s) = \frac{\mu}{s^2} \rightarrow \begin{cases} M_0 = \infty \\ \varphi_0 = -\pi \end{cases}, \quad G_{1,\infty}(s) = \frac{\mu\tau'_1}{\tau_1\tau_2} \frac{1}{s^3} \rightarrow \begin{cases} M_\infty = 0 \\ \varphi_\infty = -\frac{3}{2}\pi \end{cases}$$

The parameters Δ_τ and Δ_p are

$$\Delta_\tau = \tau'_1 - (\tau_1 + \tau_2) \quad \Delta_p = -\frac{1}{\tau'_1} - \left(-\frac{1}{\tau_1} - \frac{1}{\tau_2} \right).$$

⁴In particular, some of the transfer functions reported in [3], Tab. 9.6, have been used.

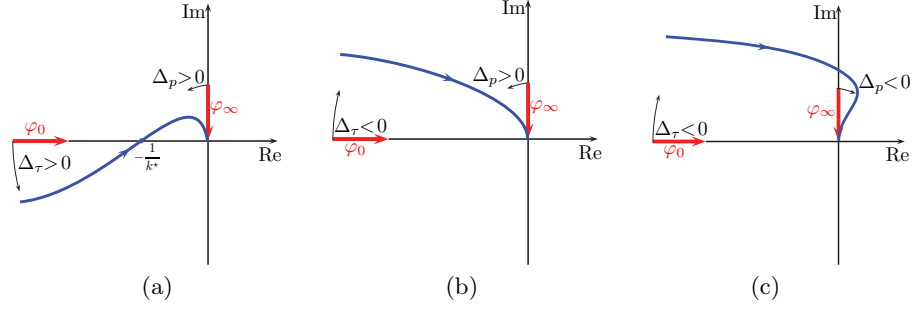


Figure 3: Nyquist plot of $G_1(s)$ for different combinations of Δ_τ and Δ_p .

Being $\varphi_\infty = -\frac{3}{2}\pi$, the value of Δ_p which determines the quadrant where the polar plot reaches the origin does not influence the stability properties of the feedback system. On the contrary, the value of Δ_τ is rather critical: $\Delta_\tau < 0$ implies that the initial segment of the polar curve is located in the second quadrant and therefore no intersections with the negative real axis occur; $\Delta_\tau > 0$ implies the polar curve starts in the third quadrant and necessarily intersects the negative real axis, see Fig. 3(a). As a consequence, by applying the Nyquist stability criterion, it comes out that $G_1(s)$ in a closed-loop configuration with a proportional regulator, whose gain is denoted by k , is unstable $\forall k$ if $\Delta_\tau < 0$ and is stable for $0 < k < k^*$ if $\Delta_\tau > 0$.

2. Consider the transfer function $G_2(s) = \mu \frac{(1 + \tau_1' s)}{s(1 + \tau_1 s)(1 + \tau_2 s)}$.

The approximating functions and the initial and final points are:

$$G_{2,0}(s) = \frac{\mu}{s} \rightarrow \begin{cases} M_0 = \infty \\ \varphi_0 = -\frac{\pi}{2} \end{cases}, \quad G_{2,\infty}(s) = \frac{\mu \tau_1'}{\tau_1 \tau_2} \frac{1}{s^2} \rightarrow \begin{cases} M_\infty = 0 \\ \varphi_\infty = -\pi \end{cases}$$

The parameters Δ_τ and Δ_p are

$$\Delta_\tau = \tau_1' - (\tau_1 + \tau_2), \quad \Delta_p = -\frac{1}{\tau_1} - \left(-\frac{1}{\tau_1} - \frac{1}{\tau_2} \right)$$

For $\Delta_\tau < 0$, the polar plot starts from third quadrant along the vertical asymptote $\sigma_0 = \mu \Delta_\tau$ and the final segment approaches the origin: a) from the third quadrant when $\Delta_p > 0$, see Fig. 4(a); b) from the second quadrant when $\Delta_p < 0$, see Fig. 4(b). The two cases are completely different: in case (a) the system $G_2(s)$ in a feedback configuration is stable for any $k > 0$, while in case (b) the

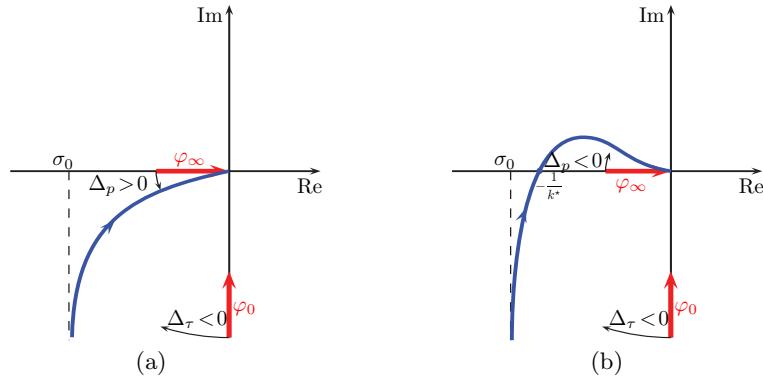


Figure 4: Nyquist plots of $G_2(s)$ for $\Delta_\tau < 0$ and $\Delta_p > 0$ (a) or $\Delta_p < 0$ (b).

stability is guaranteed only for $0 < k < k^*$. Note that the simple knowledge of the two parameters Δ_τ and Δ_p allows to obtain a qualitative plot of the polar curve that can be used to correctly predict the stability of the feedback system. The numerical value of k^* can be deduced by means of the Routh-Hurwitz stability criterion.

It is worth noticing that the plots obtained with the `nyquist` function of the Matlab Control Toolbox of the following two transfer functions:

$$G_{2,a}(s) = \frac{20(\frac{1}{10}s + 1)}{s(s+1)(\frac{1}{20}s + 1)}, \quad G_{2,b}(s) = \frac{20(\frac{1}{10}s + 1)}{s(\frac{1}{3}s + 1)(\frac{1}{2}s + 1)}$$

may be very similar. For function $G_{2,a}(s)$ the values of the two parameters are $\Delta_\tau = -0.95 < 0$ and $\Delta_p = 11 > 0$; for function $G_{2,b}(s)$ the values of the two parameters are $\Delta_\tau = -0.73 < 0$ and $\Delta_p = -5 < 0$. Only a proper magnification of the polar plot obtained by Matlab allows to establish whether an intersection with the negative real axis exists or not, see Fig. 5(c) and 5(d).

In case $\Delta_\tau > 0$ and $\Delta_p > 0$, the vertical asymptote for $\omega \rightarrow 0^+$ is located in the fourth quadrant, while for $\omega \rightarrow \infty$ the polar curve approaches the origin from third quadrant, tangent to the negative real axis, see Fig. 6(a). As a consequence, no intersections with the real axis exist, and the application of the Nyquist stability criterion leads us to conclude that, under these conditions, the system $G_2(s)$ with a feedback control is stable $\forall k > 0$. Note that a simple curve drawn by joining the initial and the final segments found with the proposed

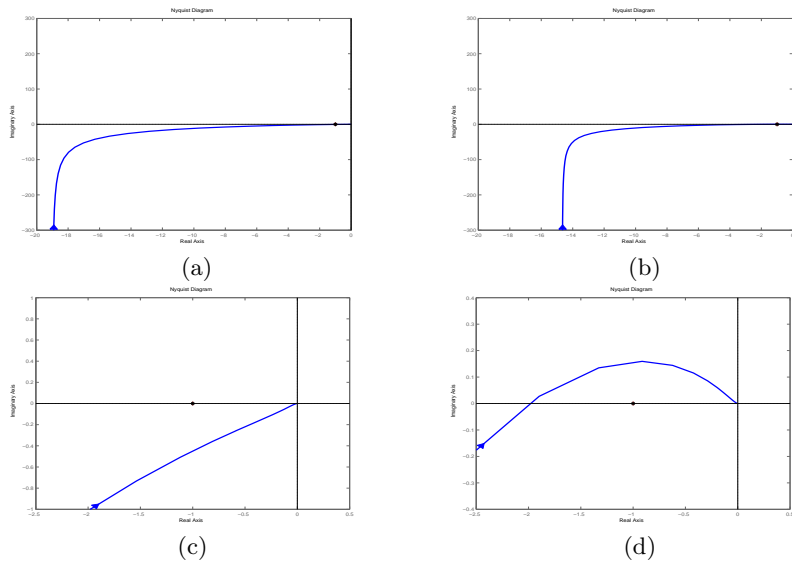


Figure 5: Matlab plots of the polar curves $G_{2,a}(s)$ ($\Delta\tau < 0$ and $\Delta_p > 0$) (a) and $G_{2,b}(s)$ ($\Delta\tau < 0$ and $\Delta_p < 0$) (b) and magnification about the origin of the polar curves (c), (d).

methods based on Δ_τ and Δ_p is able to well reproduce the real diagram, see Fig. 6(b) where the polar plot of $G_{2,c}(s) = \frac{10(s+1)}{s(s+2)(s+3)}$ obtained with Matlab is reported. The last case for system $G_2(s)$, that is $\Delta_\tau > 0$ and $\Delta_p < 0$, cannot occur with any combination of τ'_1 , τ_1 and τ_2 .

Finally, it is worth noticing that, as mentioned in the introduction, the use of parameters Δ_τ and Δ_p , together with the well-known methods such as circle criterion [7], Popov criterion [7] or describing function method [8], may be conclusive to assess the stability of the LTI system $G(s)$ when connected in a feedback configuration with a static nonlinearity. Consider, for example, the system $G_2(s)$ in Fig. 7 connected in feedback with the saturation function $y = y(x)$ with slope m . Without a precise drawing of the Nyquist plot, the circle criterion cannot be used to study the stability of the system. As a matter of fact, a sufficient condition for the absolute stability of the feedback system is that the Nyquist plot of $G_2(s)$ does not touch the critic circle that in this case is the half-plane to the left of the vertical line $\sigma = -\frac{1}{m}$. Unfortunately, this condition cannot be assured only on the basis of the knowledge of two parameters Δ_τ and Δ_p and of the possible intersections with the negative real axis. On the contrary, the

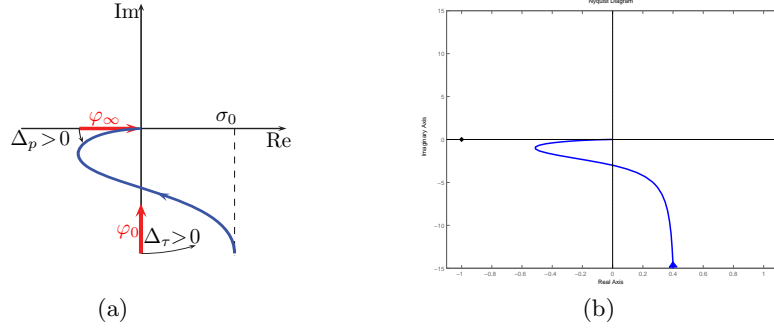


Figure 6: Nyquist plot of $G_2(s)$ for $\Delta_\tau > 0$ and $\Delta_p > 0$ (a) and Matlab plot of $G_{2,c}(s) = \frac{10(s+1)}{s(s+2)(s+3)}$ (b).

Popov Criterion assures that when $\Delta_p < 0$ the system of Fig. 7 is absolutely stable. In fact, in this case, the Popov plot $\text{Re}\{G_2(j\omega)\} + j\omega \text{Im}\{G_2(j\omega)\}$ does not intersect the real axis and therefore it is always possible to find a line of proper slope passing through the point $-\frac{1}{m} + j0$ which does not touch the Popov plot. Similar conclusions can also be obtained with the describing function method. The describing function $F(X)$ of the saturation function $y = y(x)$ in Fig. 7 is positive real, and therefore the curve $-\frac{1}{F(X)}$, for $0 \leq X \leq \infty$, belongs to the real negative axis. If $\Delta_p > 0$ the Nyquist plot of $G_2(s)$ does not intersect the negative real axis and therefore no oscillations can appear in the feedback system. Conversely, if $\Delta_p < 0$ the Nyquist plot of $G_2(s)$ intersects the negative real axis at point $-\frac{1}{k^*}$, and therefore two different situations may occur: if $m > k^*$, as shown in Fig. 8(a), an intersection between curves $G_{2,b}(j\omega)$ and $-1/F(X)$ exists and a stable persistent oscillation is present in the system, see Fig. 8(c); on the contrary, if $m < k^*$ no intersections and no oscillations exist in the feedback system, see Fig. 8(b) and Fig. 8(d).

3. In order to show that the computation of the two parameters Δ_τ and Δ_p can be easily performed even if the time-constants of the system, or equivalently the poles and zeros, are unknown, the transfer function

$$G_3(s) = \frac{1200(s+1/3)(s+1/2)}{s(1+0.5s)(50s^3+506s^2+60.1s+1)}$$

is considered [5]. Note that $G_3(s)$ is written in a mixed form (time-constants,

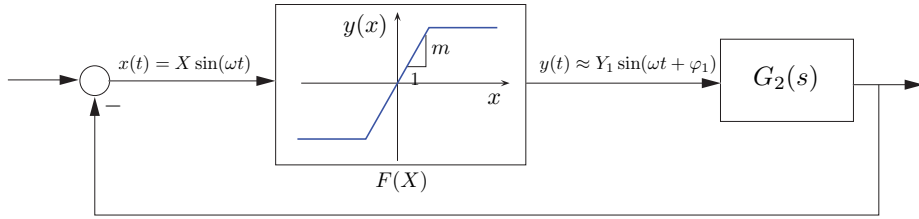


Figure 7: Feedback connection of the linear system $G_2(s)$ and the static nonlinearity $y(x)$ (saturation function) with describing function $F(X)$.

pole-zero and polynomial). By using (5) and (11), the values of Δ_τ and Δ_p are

$$\Delta_\tau = 3 + 2 - (0.5 + 60.1) = -55.6 < 0, \quad \Delta_p = \frac{1}{0.5} + \frac{506}{50} - \left(\frac{1}{3} + \frac{1}{2}\right) = 11.29 > 0$$

Since $\varphi_0 = -\frac{\pi}{2}$, $\varphi_\infty = -\frac{3\pi}{2}$ and $\Delta\varphi = -\pi$, the polar curve starts from the third quadrant and ends in the second one, see Fig. 9. Therefore, the simple analysis based only on initial and final segments leads us to conclude that at least one intersection with the negative real axis exists, and the plot of Fig. 9(a) would be the result. Indeed a deeper analysis, based for instance on Routh-Hurwitz stability criterion, shows that the transfer function with a proportional feedback control is stable for $0 \leq k \leq k_1^* = 0.0013$ and $k_2^* = 0.0713 \leq k \leq k_3^* = 2.861$. As a consequence, see Fig. 9(b), there are three intersections with the real axis: $\sigma_1 = -\frac{1}{k_1^*} = -769.23$, $\sigma_2 = -\frac{1}{k_2^*} = -14.02$ and $\sigma_3 = -\frac{1}{k_3^*} = -0.3495$. Note that the Nyquist plot obtained with the Matlab function does not highlight the presence of intersections with the real axis, see Fig. 10(a), and only with a progressive enlargement of the plot about the origin it is possible to detect such points, see Fig. 10(b) and Fig. 10(c).

5. Conclusion

In this paper, the use of two novel parameters Δ_τ and Δ_p for improving and simplifying the standard techniques for qualitative drawing of the Nyquist plot is proposed. The two parameters can be computed with simple calculations involving only additions and divisions, and in many cases are sufficient to draw qualitative plots that provide all the information needed for assessing the

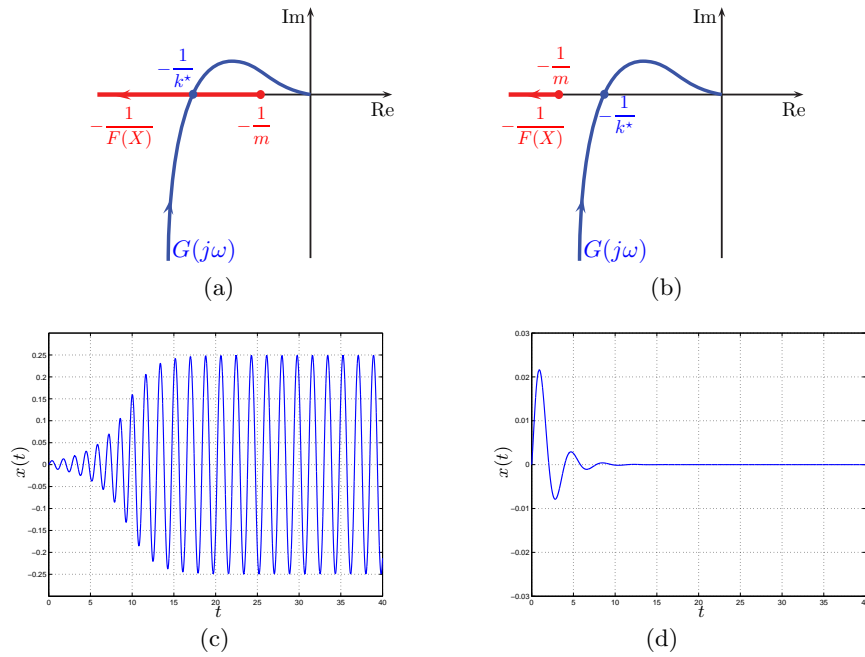


Figure 8: Nyquist plot of $G_{2,b}(s)$ and plot of $-1/F(X)$ for $m > k^*$ (a) and $m < k^*$ (b). Impulse response of the closed-loop system for $m = 1$ (c) and $m = 0.1$ (d).

stability of linear and nonlinear systems with a feedback control. Moreover, the two parameters can be helpful for a correct interpretation of the Nyquist plots obtained with numerical programs, such as Matlab. As a matter of fact, when the range of variation of the module of the polar plot is very large the plots obtained with numerical methods may hide some fundamental details, like the intersections with the real axis. A simple analysis based on Δ_τ and Δ_p can suggest if any intersection exists, and if it is necessary to increase the level of magnification of the plot to show them.

- [1] G. F. Franklin, D. J. Powell, A. Emami-Naeini, Feedback Control of Dynamic Systems, 4th Edition, Prentice Hall PTR, Upper Saddle River, NJ, USA, 2001.
- [2] B. C. Kuo, F. Golnaraghi, Automatic Control Systems, 9th Edition, John Wiley & Sons, Inc., New York, NY, USA, 2002.

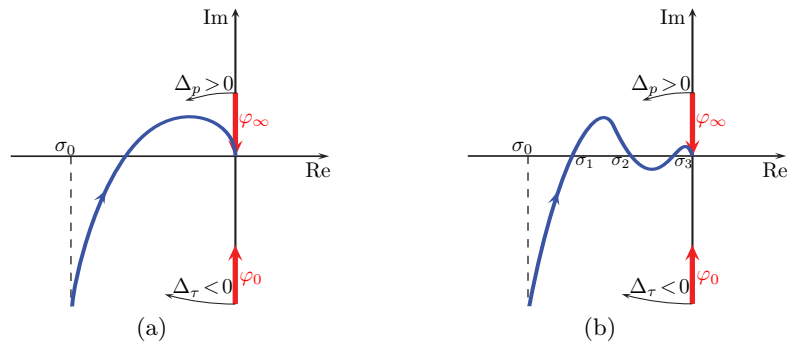


Figure 9: Nyquist plot of $G_4(s)$ for $\Delta_\tau < 0$ and $\Delta_p > 0$

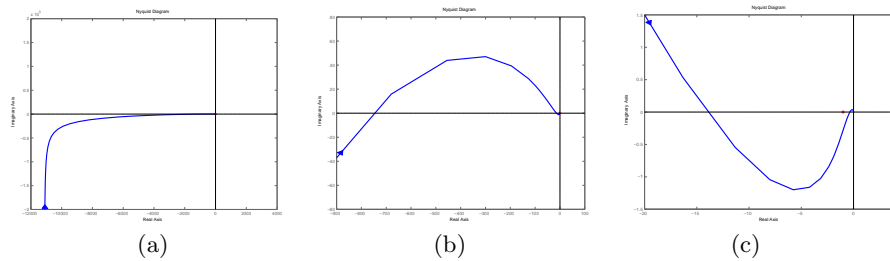


Figure 10: Polar plot of $G_4(s)$ obtained with Matlab for different levels of magnification.

- [3] R. C. Dorf, R. H. Bishop, Modern Control Systems, 11th Edition, Prentice Hall PTR, Upper Saddle River, NJ, USA, 2008.
- [4] P. Ferreira, Concerning the Nyquist plots of rational functions of nonzero type, Education, IEEE Transactions on 42 (3) (1999) 228–229.
- [5] T. Andresen, A logarithmic-amplitude polar diagram, Modeling, Identification and Control 22 (2) (2001) 65–72.
- [6] R. Zanasi, F. Grossi, Open and closed logarithmic nyquist plots, in: Proceedings of 2014 European Control Conference (ECC), 2014.
- [7] H. Khalil, Nonlinear Systems, Prentice Hall PTR, 2002.
- [8] K. J. Astrom, R. M. Murray, Feedback Systems: An Introduction for Scientists and Engineers, Princeton University Press, Princeton, NJ, USA, 2008.